Trap filter using bracelet resonator

Bastien Roucariès, Pascal Griesmar, Stéphane Serfaty

21ème Colloque International et Exposition sur la Compatibilité ÉlectroMagnétique (CEM 2023)

Trap filter using bracelet resonator

Bastien Roucariès[1], Pascal Griesmar[1], and Stéphane Serfaty[1]

[1]SATIE Laboratory, 95000 Cergy, France, bastien.roucaries@ens-paris-saclay.fr
[2]SATIE Laboratory, 95000 Cergy, France, pascal.griesmar@cyu.fr
[3]SATIE Laboratory, 95000 Cergy, France, stephane.serfaty@cyu.fr

Résumé

The bracelet resonator is a low cost resonator made from printed circuit technology. The resonance frequency was first computed in [1], unfortunately the whole transfert function of the resonator was not yet computed, particularly coupling with external circuit.

The coaxial shape of this kind of resonator may render it particularly suitable as a trap filter for coaxial line

Unfortunately, for these resonators, the extremely small metalisation depth compared to radius renders the simulation by finite element (FEM) extremely hard (slow) and memory consuming. Moreover, the simulation should be carried in 3D due to asymmetric nature of the gaps, and the finite height, increasing the complexity. Time domain methods are not well suited due to high quality coefficient of this kind of resonator. Thus a physical approximation of this resonator will be carried.

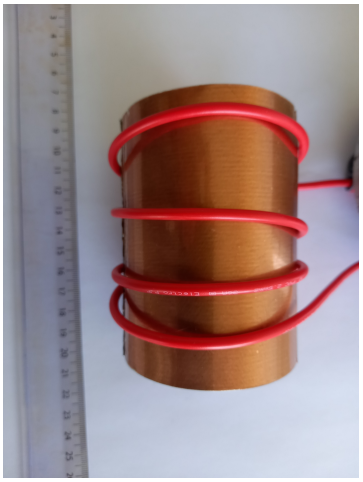

Figure 1: Use of this kind of resonator as a quick and easy to use trap filter around 46 MHz

I Model

This sensor is mainly used in NMR field for increasing signal to noise ratio (SNR) and is used for instance for imaging small animals or determining in-vivo clinical parameters [2, 3, 4]. This resonator could be also use as a dielectric sensor [5, 6, 7, 8] or as a wireless coupler for viscous fluids monitoring [9]. This kind of resonator is also used as a quick and easy to use trap filter (see figure 1 for a trap filter used for rejecting a signal around 46 MHz), unfortunately in this case the design of this kind of filter is only based on a single resonator element and without taking in account the loss of the resonator.

The goal of this paper, is to build a model of the resonator, and a in second time build an electrical distributed model, that will be solved by analytical modified nodal analysis (MNA). In order to study this kind of resonator and in order to simplify the analysis we could as usual in the electromagnetic compatibility field consider that the resonator is excited by a small probe.

The resonator ($\mathcal{R}$) and the excitation probe ($\mathcal{P}$) are coupled thought a magnetic coupling. The resonator consist of two concentric sheets of metal (rings), $\mathcal{S}_+$ for the exterior one (interior radius of $\mathcal{S}_+$ sheet is $r_+ = r_0(1+\delta r)$) and $\mathcal{S}_-$ for the interior one (external radius of $\mathcal{S}_-$ sheet is $r_- = r_0(1-\delta r)$), with r_0 is the arithmetic mean of sheet radius: $2r_0 = r_+ + r_-$. Sheets are separated by a dielectric layer of relative permittivity ε_r and loss tangent δ_d. Metalisation depth of each sheet is $2\Xi r_0$ and conductivity of metal is σ. The height of resonator is $2h$ and is linked to the mean radius by the relation $h = \zeta r_0$. Two gaps on the sheet are manufactured at $\theta = \pm\pi/2$ respectively for $\mathcal{S}_+$ and $\mathcal{S}_-$. The metalisation breaks dimension at the gap are negligible.

In order to simplify the computation, we could also define the half-diagonal (normalised) of the coil, defined by $\ell_\pm = \sqrt{(1 \pm \delta r)^2 + \zeta^2}$.

A summary of geometric concepts is given by the figure 2.

The probe is considered sufficiently small to be modelled as an inductive (lossy) lumped element (thus an impedance $Z_p = sL_P + R_P$ with s the

†This paper is dedicated to the memory of the late Professor Jean-Yves le Huerou 1959-2020.

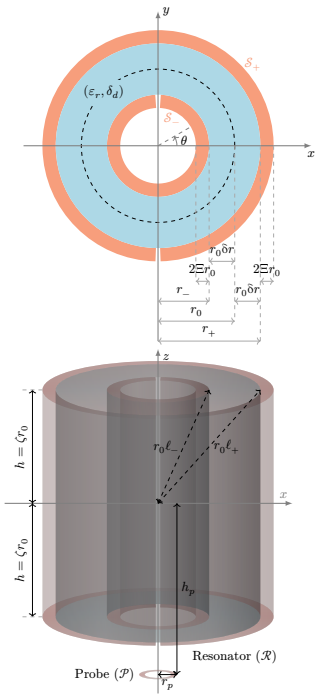

Figure 2: Schematic diagram of resonator including dimensioning (not to scale)

laplace variable).

Therefore, the problem can be simplified using reciprocity and superposition. Instead, of studying the scattered field by the resonator [11, 12] we study the vector potential vector $\vec{A}$ generated by two arbitrary physical current distribution $\vec{J}_+(\theta, z)$ along $\mathcal{S}_+$ sheet and $\vec{J}_-(\theta, z)$ along $\mathcal{S}_-$ sheet.

Following a classical approach [10], the current density is decomposed in two orthogonal modal current density $\vec{J}_e(\theta, z) = {}^1\!/\!_2(\vec{J}_+ + \vec{J}_-)$ called the antenna current density or common mode current (even) and $\vec{J}_o(\theta, z) = {}^1\!/\!_2(\vec{J}_+ - \vec{J}_-)$ called a differential (odd) current density. The ratio between the two current is fixed by closure condition particularly along the gaps where $(\vec{J}_e + \vec{J}_o) \cdot \vec{e}_n = 0$ (with $\vec{e}_n$ a vector normal to the gap). Unfortunatly this decomposition is valid only for lossless model, losses need the real current and voltage and not modal current, but nevertheless could be generally reintroduced at the end of the study as a pertubation of the lossless model.

1 Common mode current

The current $\vec{J}_e$ could be approximated by the means term [13], if the loop circonference is less than ${}^{\lambda_0}\!/\!_{16}$ with λ_0 the free space wavelength. Experimental evidence for small loop support this view [14] and support that error in this case is inferior to 1%.

The dielectric sheet effect could be neglected for antenna currents. Indeed, potential difference between the two sheets is constant for antenna current mode under the previous assumption of constant current density. Moreover under previous assumption the common mode current is azimuthal.

The antenna current contribution is thus equivalent, to two lossy coupled coils, coupled magnetically to the probe. The inductance is computed using classical formulæ of sheet inductance, including mutual inductance between the two sheets[15, 16, 17].

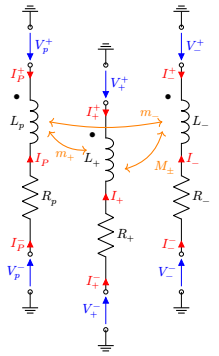

Figure 3: Equivalent common mode circuit.

Losses could be introduced by a serial resistance (denoted by $R_\pm$ for $\mathcal{S}_\pm$) taking in account conductive loss but need to take in account the real current as seen in the introduction.

Coupling between the probe and the two sheet of current could be estimated by using Groover formulae and some reasonable approximation and could be represented by a mutual inductance $m_\pm$.

Thus the two sheets for antenna current could be modelled by a complex serial lumped impedance $Z_\pm = sL_\pm + R_\pm$. Coupling to the sheets from the probe are achieved by small mutual impedance $m_\pm$.

The equivalent circuit, of this mode, is shown in figure 3.

2 Differential mode current

The differential mode is modelled by a transmission line, exactly by a paired strips line [19, 20]. This structure is electrically related to a microstrip line [20, 21], and thus the current is mainly azimuthal. The propagation mode of this current is quasi TEM. The characteristic impedance Z_L of the paired line of height $2r_0\delta r$ is twice the one of a microstrip of height $r_0\delta r$. The propagation characteristic of the line are computed by first computing relative effective dielectric constant of the line ε_{er} defined $\varepsilon_{er} = {}^{Z_L^2}\!/\!_{Z_1^2}$, with Z_1 the impedance of the same line filled with vacuum instead of dielectric [22]. Then the propagation constant β is then computed by using well known formula $\beta = {}^{\omega\sqrt{\varepsilon_{er}}}\!/\!_c$. Microstrip impedance needed for the previous computation is computed using classical expressions of Wheeler [23]. If needed empirical formulæ of Hammerstad could be used in order to improve precision and take in account the dispersion [24].

Losses are computed using classical formulæ for microstrip but doubling the loss of the strip and not taking in account the loss due to ground plane [25, 23]. Dielectric loss are computed using classical formulæ for microstrip line but doubling the losses [23, 26]. Then the attenuation constant α is computed using classical transmission line formulæ. Note that conductive loss should not be included here in order to avoid a double accounting with antenna current losses.

These lines could also be modelled using $R = Z_L^{-1}\coth(\gamma\ell)$ the reflection coefficient at input, $T =$

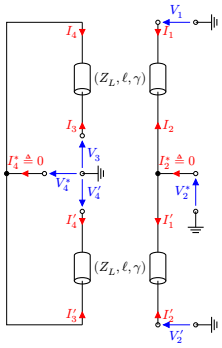

Figure 4: Equivalent differential mode circuit

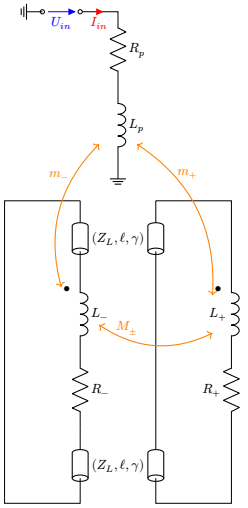

Figure 5: Electrical schematic of the resonator and the probe.

$Z_L^{-1}\,\mathrm{csch}(\gamma\ell) = Z_L^{-1}(\coth\gamma\ell/2 - \coth\gamma\ell)$ the transmission coefficient between input and output

Coupling between this mode and the probe is negligible due to small δr.

The equivalent circuit, of this mode, is shown in figure 4.

In order to ease notation for the next section, let define means parameters $\tilde{x}$ of $x_\pm$ by using arithmetic means ($2\tilde{x} = x_+ + x_-$), thus $2\tilde{L} = L_+ + L_-$, $2\tilde{R} = R_+ + R_-$, $2\tilde{Z} = Z_+ + Z_- = 2s\tilde{L} + 2\tilde{R}$, $2\tilde{m} = m_+ + m_-$.

3 Resonator model

Using models from the previous section a electrical schematic of the resonator could be derived. Antenna current is represented using three coupled coils whereas the differential current is represented by two section of length ℓ of a four terminal transmission line. The electrical schematic of the resonator is given by the figure 5. Resolution of this schematic could be carried by using block decomposition using MNA of the whole schematic.

Coupling coil to line leads along the closure condition at the gap, leads to the following system by using current conservation law:

$$\begin{pmatrix} 0 \\ 0 \\ 0 \\ \frac{I_P^{+*} - I_P^{-*}}{2} \\ \frac{I_+^{+*} - I_+^{-*}}{2} \\ \frac{I_-^{+*} - I_-^{-*}}{2} \end{pmatrix} = \mathbf{M}'' \begin{pmatrix} I_P \\ I_+ \\ I_- \\ V_P^+ - V_P^- \\ V_+^+ - V_+^- \\ V_-^+ - V_+^- \end{pmatrix} \tag{1}$$

With M'' the quasi symmetric matrix using the following means parameters defined by $m_\pm = \tilde{m}(1 \pm \delta\tilde{m})$, $2\tilde{A} = A_+ + A_- = 2(\tilde{Z} + 2RZ_L^2)$, and $\tilde{A}(1 \pm \delta\tilde{A}) = \tilde{Z}(1 \pm \delta\tilde{Z}) + 2RZ_L^2$, and defined by

$$\mathbf{M}'' = \begin{pmatrix} 0 & 1 & 0 & 0 \\ -1 & Z_p & s\tilde{m}(1+\delta\tilde{m}) & s\tilde{m}(1-\delta\tilde{m}) \\ 0 & s\tilde{m}(1+\delta\tilde{m}) & \tilde{A}(1+\delta\tilde{A}) & B \\ 0 & s\tilde{m}(1-\delta\tilde{m}) & B & \tilde{A}(1-\delta\tilde{A}) \end{pmatrix}$$

4 Input impedance

By Cramer's rule input impedance is defined by $Z_{\text{in}} = {}^{U_{\text{in}}}\!/_{I_{\text{in}}} = {}^{\det \mathbf{M}_1''}\!/_{\det \mathbf{M}''} = {}^{N}\!/_{D}$, with $\mathbf{M}_1''$ the $\mathbf{M}''$ matrix with first column replaced by vector $(1,0,0,0)^\top$. By element computation $\det \mathbf{M}'' = D = \tilde{A}^2(1 - \delta\tilde{A}^2) - B^2$. Therefore:

$$Z_{\text{in}} = Z_p - s^2 \frac{2\tilde{m}^2\left[\tilde{A} - B + \delta\tilde{m}^2(\tilde{A}+B) - 2\tilde{A}\delta\tilde{A}\delta\tilde{m}\right]}{\tilde{A}^2(1-\delta\tilde{A}^2) - B^2}$$

This impedance could be written as:

$$Z_{\text{in}} = Z_p - \frac{s^2\tilde{m}^2}{Z_Q}$$

This equation correspond to a coupled coil impedance,with Z_Q the internal (unloaded) resonator impedance:

$$Z_Q = {}^1\!/_2 \frac{(\tilde{A}-B)(\tilde{A}+B) - \tilde{A}^2\delta\tilde{A}^2}{\tilde{A} - B + \delta\tilde{m}^2(\tilde{A}+B) - 2\tilde{A}\delta\tilde{A}\delta\tilde{m}} \tag{2}$$

Using Taylor expansion near $(0,0)$ for $(\delta A, \delta\tilde{m})$, until order 3:

$$Z_Q = \tfrac{1}{2}(\tilde{A}+B)\left[1 - \frac{(\delta\tilde{m}(\tilde{A}+B) - \tilde{A}\delta\tilde{A})^2}{(\tilde{A}+B)(\tilde{A}-B)} + o\Big(\|(\delta\tilde{A}, \delta\tilde{m})\|_2^3\Big)\right] \tag{3}$$

Let simplify a $\tilde{A}+B$ terms using half angle formulae:

$$\begin{aligned} \tilde{A} + B &= \tilde{Z} + 2RZ_L^2 + sM_\pm - 2TZ_L^2 \\ &= s(\tilde{L} + M_\pm) + \tilde{R} + 2Z_L \coth\gamma\ell/2 \end{aligned}$$

Let now simplify $A - B$:

$$\begin{aligned} \tilde{A} - B &= \tilde{Z} + 2RZ_L^2 - sM_\pm + 2TZ_L^2 \\ &= s(\tilde{L} - M_\pm) + \tilde{R} + \frac{2Z_L[\cosh(\gamma\ell)-1]}{\sinh(\gamma\ell)} \\ &= s(\tilde{L} - M_\pm) + \tilde{R} + 2Z_L \tanh\gamma\ell/2 \end{aligned}$$

Thus until order 2, the following impedance and main result of this paper:

$$Z_Q \simeq \tfrac{1}{2}\left[s(\tilde{L} + M_\pm) + \tilde{R} + 2Z_L \coth\gamma\ell/2\right] \tag{4}$$

Experimental measurement of this kind of resonator is given in figure 6.

II Conclusion

A new model including losses and coupling was developed for a bracelet resonator. This new development is expected to enable easy design of new trap filter for coaxial lines or twin-lead line using well known theory of microwave filters. New development will be carried in order to evaluate more precisely the losses of this kind of resonator, and carrying an optimisation along the geometrical parameters.

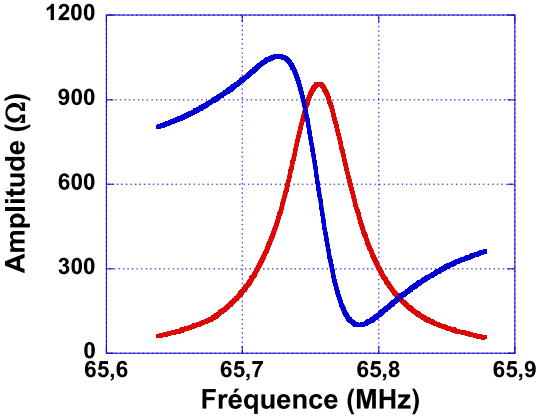

Figure 6: Measurement of a typical resonator

References

[1] P. Gonord, S. Kan, A. Leroy-Willig, and C. Wary, *"Multigap parallel-plate bracelet resonator frequency determination and applications"*, Review of Scientific Instruments, vol. 65, no. 11, pp. 3363–3366, 1994.

[2] L. Darrasse and J.-C. Ginefri, *"Perspectives with cryo- genic RF probes in biomedical MRI"* Biochimie, vol. 85, no. 9, pp. 915–937, 2003.

[3] A. Watrin-Pinzano, J.-P. Ruaud, P. Olivier, et al., "Effect of proteoglycan depletion on T2 mapping in rat patellar cartilage", Radiology, vol. 234, no. 1, pp. 162–170, 2005.

[4] J. Issartel, Y. Voituron, V. Odagescu, et al., *"Freezing or supercooling: How does an aquatic subterranean crustacean survive exposures at subzero temperatures?"* Journal of Experimental Biology, vol. 209, no. 17, pp. 3469–3475, 2006.

[5] G. Masilamany, P. Y. Joubert, S. Serfaty, B. Roucaries, and Y. L. Diraison, *"Radiofrequency inductive probe for non-contact dielectric characterisations of organic medium"* Electronics Letters, vol. 50, no. 7, pp. 496– 497, Mar. 2014.

[6] T. H. N. Dinh, E. Martincic, P. Y. Joubert, and S. Serfaty, *"Monitoring of yogurt formation using a contact- less radiofrequency dielectric sensor"* in IEEE Sensors 2016, Orlando, FL, USA: IEEE, 2016.

[7] T.-H.-N. Dinh, M. Wang, S. Serfaty, and P.-Y. Joubert, *"Contactless radio frequency monitoring of dielectric properties of egg white during gelation"* IEEE Transactions on Magnetics, vol. 53, no. 4, pp. 1–7, Apr. 2017.

[8] T.-H.-N. Dinh, T. Bore, S. Serfaty, and P.-Y. Joubert, *"Non-invasive evaluation of yogurt formation using a contactless radiofrequency inductive technique,"* in Electromagnetic Nondestructive Evaluation (XX) (Studies in Applied Electromagnetics and Mechanics), H. Geirinhas Ramos and A. Lopes Ribeiro, Eds., Studies in Applied Electromagnetics and Mechanics. Amsterdam, The Netherlands: IOS Press, 2017, vol. 42, pp. 298–305.

[9] N. Wilkie-Chancellier, S. Serfaty, P. Griesmar, Y. Le Diraison, and J.-Y. Le Huérou, *"Inductive magneto-acoustic technique for viscous fluids monitoring"* in Ultrasonics Symposium (IUS), 2011 IEEE International, IEEE, Orlando, FL, USA, 2011, pp. 1107–1110

[10] R. E. Collin, *Fundation for Microwave Engineering* (The IEEE press serie on Electromagnetics Wave Theory), 2nd ed. IEEE, 2001.

[11] A. Vukicevic, F. Rachidi, M. Rubinstein, and S. V. Tkachenko, "On the evaluation of antenna-mode currents along transmission lines" IEEE Transactions on Electromagnetic Compatibility, vol. 48, no. 4, pp. 693–700, Nov. 2006.

[12] M. Heggo, X. Zhu, Y. Huang, and S. Sun, *Study of high frequency conversion from excited antenna mode to differential mode current at the transmission line terminals* in 12th IEEE Asia Pacific Wireless Communications Symposium (IEEE VTS APWCS 2015), Nanyang Technological University, Singapore: IEEE, Aug. 2015.

[13] L.-W. Li, M.-S. Leong, P.-S. Kooi, and T.-S. Yeo, *"Exact solutions of electromagnetic fields in both near and far zones radiated by thin circular-loop antennas: A general representation"* IEEE Transactions on Antennas and Propagation, vol. 45, no. 12, pp. 1741–1748, 1997.

[14] R. W. P. King, *Tables of antenna characteristics* New York: Springer, 1971

[15] L. Lorenz, *Ueber die fortpflanzung der electricität"* In German, Annalen der Physik und Chemie, vol. 243, no. 6, pp. 161–193, 1879.

[16] M. Romanosky, *"Introduction au calcul des inductances"* In French, Travaux et Mémoires du Bureau International des Poids et Mesures, vol. 20, 1944.

[17] R. Cazenave, *"Inductance mutuelle de deux bobines cylindriques circulaires coaxiales à une couche de spires jointives en fil fin"* Annales des Télécommunications, vol. 11, no. 9, pp. 174–179, 1956.

[18] L. Cohen, *"An exact formula for the mutual inductance of coaxial solenoids"* Bulletin of the Bureau of Standards, 1907.

[19] B. C. Wadell, *"Transmission Line Design Handbook"* Norwood, MA: Artech House, 1991.

[20] H. A. Wheeler, *"Transmission-line properties of parallel strips separated by a dielectric sheet"* IEEE Transactions on Microwave Theory and Techniques, vol. 13, no. 2, pp. 172–185, Mar. 1965.

[21] R. Schinzinger and P. A. Laura, *"Conformal mapping, methods and applications"* 2nd ed. Dover, 2003

[22] M. V. Schneider, *"Microstrip lines for microwave integrated circuits"* Bell System Technical Journal, vol. 48, no. 5, pp. 1421–1444, May 1969.

[23] H. A. Wheeler, *"Transmission-line properties of a strip on a dielectric sheet on a plane"* IEEE Transactions on Microwave Theory and Techniques, vol. 25, no. 8, pp. 631–647, Aug. 1977

[24] E. Hammerstad and Ø. Jensen, *Accurate models for microstrip computer-aided design* in IEEE MTT-S International Microwave symposium Digest, Washington, D.C., USA: IEEE, May 1980, pp. 407–409

[25] R. A. Pucel, D. J. Masse, and C. P. Hartwig, *"Losses in microstrip"* IEEE Transactions on Microwave Theory and Techniques, vol. 16, no. 6, pp. 342–350, Jun. 1968,

[26] M. V. Schneider, *"Dielectric loss in integrated mi- crowave circuits"* Bell System Technical Journal, vol. 48, no. 7, pp. 2325–2332, Sep. 1969